Journal of Polymer Research (2023) 30:359
https://doi.org/10.1007/s10965-023-03746-y

ORIGINAL PAPER

Optical development and density modification dependence in poly (methyl methacrylate) reinforced with borax microparticles

Yusuf Yigit[1] · Fuat Berke Gul[1,2] · Candidate Hilal Macun[1] · Nilgun Baydogan[1]

Received: 20 April 2023 / Accepted: 15 August 2023 / Published online: 25 August 2023

Abstract

The synthesis of the poly (methyl methacrylate) composite containing borax decahydrate microparticles at two different concentrations (such as 5 and 10 wt %) was significant to derive amphibious features (such as wettability and hydrophilicity) by using the atom transfer radical polymerization (ATRP) method. The composite has provided an optimum optical identification level as borax decahydrate (as the filler particle) was used to develop the optical modification in this lightweight composite. The optical development has provided a homogeneously spread of light at the surface and ideal identification conditions in the working area as the modified optical properties were solved through several material problems and developed to improve its amphibious movement in corrosive ambient. Optical identification (by using colour coordinates) has been generated with the development of the lighting homogeneity allowing the surface of the composite product to come to the fore as the result that the surface roughness increased slightly with the rise of the borax microparticle amount. The control of the borax addition has provided the modification of the amphibious design with the rise of wettability to develop multifunctional applications. The surface of this composite has reached sligitly a more hydrophilic feature with the modification of the surface morphology. The decrease of optical transmittance by borax addition in PMMA synthesis has been enhanced with the slight modification of the amphibious design of the composite.

Keywords Composite · Polymer · Synthesis · Surface · Reinforcement

Introduction

Poly (methyl methacrylate) (PMMA) is the synthetic glass. It is used as a lightweight thermoplastic as the result of the modification of its high temperature resistance, high optical transparency, high strength and optimum mechanical performance (with several advantages based on acrylic polymer industry) [1, 2]. The PMMA is resistant to sudden temperature changes, shock effects, and UV rays [3–8]. Several polymer composites (such as PMMA) are combined with boron and its compounds [9–11]. The use of boron nitride (BN) reinforced PMMA polymer composites is encountered in the literature [12–15]. The boron compounds improve the properties of PMMA (for example, borax decahydrate ($Na_2B_4O_7.10H_2O$ -sodium tetraborate decahydrate)). The use of borax decahydrate (as an alkaline salt) is preferred as it has excellent flow (with buffering properties produced by refining tincal ore in powder and crystal form) in polymer solution at the polymerization [16]. Borax has white colour and it can be used in industrial areas including glass and ceramic industries as a soft abrasive in industrial cleaners [17]. Borax decahydrate is a suitable agent for the utilization of flame retardancy, corrosion prevention, water softening and water treatment. Its use is preferred as the high-performance cleaning agent in the innovative antibacterial amphiphilic processes (such as surface cleaning and removal of heavy dirt) [18–20].

The extreme ambient conditions in sea require reliable features including lightweight and amphibious properties (such as the PMMA composite modified by borax) at the systems in the sea. The improvement of composite by borax provides its effective use as the result of its development of the working performance (such as at marine subsurface to examine the seabed for the preventing of the accidents resulting with oil/gas pollution) at

✉ Nilgun Baydogan
dogannil@itu.edu.tr

[1] Energy Institute, Istanbul Technical University, Ayazaga Campus, Istanbul 34469, Turkey

[2] Department of Energy Science & Technologies, Turkish - German University, Istanbul, Turkey

the equipment. The use of the PMMA based composite at real-time automatic unmanned underwater monitoring vehicles (RT–AUVs) has some logic advantages. The modified PMMA by borax particles supports to redesign the synthesized PMMA by ATRP method and the filler reinforcement has improved the synthesized corrosion-resistant thermoplastic PMMA structure against to salt water (seawater contains 35 g of salt, NaCl, per litre). PMMA thermoplastic (which density is similar to water density) is easy to shape in its novel applications (such as modified amphibious and optical transparent properties). PMMA can be accepted as an ideal amphibious material candidate in the development of advanced RT–AUVs. However, its requirements of the mechanical impact and thermal properties need to be improved by using several reinforcement fillers for use in aggressive environments (such as corrosive ambient) [11, 12]. Several particles can be utilized to enhance the physical features of PMMA [13, 14]. MMA has the easy polymerizability property. MMA can be used with several transition metal catalysts (copper, rhodium, ruthenium, iron, nickel and palladium) at the Atom Transfer Radical Polymerization method (ATRP) [21–23]. The catalyst has an important role for the determination of the position of atom transfer equilibrium with exchange dynamics (between dormant and active species) in ATRP method. Solvent can improve the solubility of the catalyst complex affecting the atom transfer equilibrium with the modification of the rate in the polymerization reaction [23]. ATRP is an effective method for producing controllable polymers among polymer production techniques. The polymethylmethacrylate (PMMA) synthesized by the ATRP method has the molecular weight (~ 275,000 g/mol) for the improvement of the mechanical properties in the previous study [20]. The composite system (which can move forward on land and in water) is able to prevent the vehicle from capsizing as the use of the ATRP technique supports improving the polymer's molecular weight [24]. The increase of the molecular weight (with the rise of the filler amount) provides synthesis with a satisfactory density [11, 12, 24, 25]. The molecular weight of PMMA derived by ATRP method has higher than that of industrial PMMA as the number of bonding sites present that the monomers has provided a mechanical functionality in PMMA [26–39]. The hardness value decreases to 83,6 value when the borax amount reaches to 10 wt. % [40]. The adaptation of the PMMA (used for underwater applications and several different applications such as bone based polymer as a biocompatible thermoplastic at the oncological applications etc.) is possible [1, 7, 11, 12, 18]. The modern biology considered a living cell as a kind of factory with controlled by DNA [29, 30]. PMMA/Borax hybrid composite presents several results that aim to solve the problems of the lightweight platform material (such as; use at the offshore platforms in the oil and gas sectors) [41–45]. This hybrid material (including PMMA and borax) is interpreted by specifying the state-of-the-art literature.

In this study, the dissolution problem of the borax microparticles in PMMA (as one of the main problems in the composite) has been solved with the improvement of the structural features for the amphibious properties of material that enabled it to function effectively in both aquatic ambient with corrosive features and terrestrial environments. The borax decahydrate at a maximum critical amount (at 10 wt%) was used as a key filler amount in PMMA to increase its operational efficiency in the composite. The chemical bonding structure of the composite was specified to develop the physical capabilities of the composite (involving the combination of adaptations and allowing them to function effectively in aquatic and terrestrial environments). This composite was produced by the borax addition to obtain an alternative lightweight polymer composite for the modification of corrosion-resistant properties (for more resistant to water and salty water environment at underwater). The use of the PMMA/Borax composite has offered cost-effective solutions for the control of gravity effect of water on the modified surface of this composite in harsh corrosive ambient (such as oil and gas reservoir research areas in the sea or in bloood).

Experiments

Materials

The chemicals were $C_5H_8O_2$ (Methyl Methacrylate), MMA) as the used monomer. CuBr (Copper Bromide, catalyst), $C_{16}H_{36}BrN$ (Tetra-n-butylammonium bromide, Bu4NBr, solvent), $C_6H_{11}BrO_2$ (Ethyl 2-bromoisobutyrate, EBIB, initiator), $C_9H_{23}N_3$ (1,1,4,7,7- Pentamethyldiethylenetriamine, PMDETA, ligand) and $Na_2B_4O_7.10H_2O$ (borax decahydrate, additive) were utilized at the synthesis of the composite (to derive as the advanced engineering material). The preparation of the chemicals for the synthesis was performed by using a two-handed atmos-bag filled in argon.

Fabrication

Bu_4NBr (3.76 mmol) and CuBr (0.47 mmol) were put in the MMA monomer (0.282 mol) at various quantities of borax decahydrate (5 and 10 wt. %) with Bu_4NBr. Methyl methacrylate (MMA) was added to the mixture in argon. PMDETA (0.47 mmol) was added and then the mixture has been degassed in during 30 min. The balance between the physical factors (such as the generation of the coronal layers by using MMA at the modification of the optical

features) and the modification of the dissolved borax particles (like the antibacterial amphiphiles) has been performed for the modification of the hydrophilic features in the composite. The addition of salt (CuBr) has contributed to the modification of electrostatic repulsion on the surface. EBIB (0.47 mmol) was put in this mixture to start the polymerization process. This magnetic stirrer was used at 70 °C to avoid the agglomeration of particles. The sample has been taken sensitively into a mould to complete the tempering at room temperature for the improvement of the bonds derived partially.

The high viscosity causes difficult molding of the polymer and the optimization of molecular weight is needed between 10.000–1.000.000 g/mole for the suitable molding of the polymers [20, 42, 46–49]. While the mixture has begun to solidify at the polymerization step, the mixture was poured into glass molds. Then the vacuum has been applied in 70 kPa during half an hour. Vacuum pump has provided to prevent the formation of the bubble in the polymerization step of the polymer after pouring in polymer molds. Thus, air bubbles were eliminated for the mechanically stable polymer was derived. ATRP method has provided to make more sensitive thin edges as the ATRP method has supported the controlled polymerization for the molecular weight. The optimum viscosity has been supported to obtain the suitable moulding of the polymer and the optimization of the molecular weight of the polymer. The shematic representation of the borax reinforcement at PMMA was presented in Fig. 1.

Testing for structural characterization

Structural characterizations were carried out by X-ray Diffraction (XRD), Energy Dispersive X-Ray Analysis (EDX), Scanning Electron Microscope (SEM), and Fourier Transform Infrared Spectroscopy (FTIR) Analysis. The determination of the surface morphology, the distribution of the borax on the surface of PMMA/Borax composites, and the surface images of the samples were taken by using Leica MZ 10 F model stereomicroscope. FTIR analysis was performed by using Bruker ALPHA Spectrometer and XRD results were determined by Xpert Pro model device with the conditions of 2°/min scanning speed and 40 kV voltage, 40 mA current values. SEM images and EDX analysis also were indicated by using Quanta FEG 250 model device. Thermo K-Alpha device was used to find the types of bonds formed in the samples.

Cu (Copper) (having single crystal diffraction) was used with the emission of CuKα radiation in XRD. CuKα's wavelength was 1.5418 A°. Borax crystallite sizes in PMMA/Borax based on the XRD results were determined according to Scherer Formula in Eq. (1). D is an average crystallite size, K is the shape factor (in this study is equal to 0.94), λ is a wavelength of X-Rays, β is FWHM (Full Width at Half

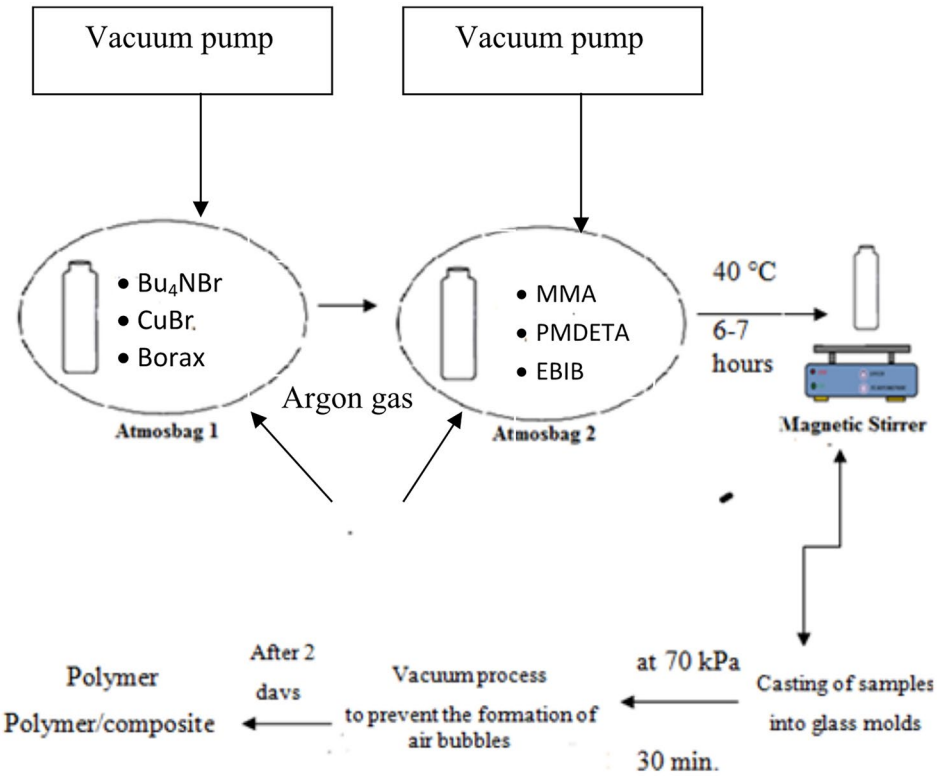

Fig. 1 Scheme of formation of PMMA/Borax composite derived by ATRP method

Table 1 Crystallite Size Values of Base PMMA, 5 and 10 wt.% PMMA/Borax

Sample	Crystallite Size (nm)
Base PMMA	32.03
%5 PMMA/Borax	51.44
%10 PMMA/Borax	60.71

Maximum) and θ_B is Bragg diffraction angle [23, 50–53]. The crystallite sizes of the specimens were shown in Table 1.

$$D = \frac{K\lambda}{\beta cos\,(\theta_B)} \quad (1)$$

Increasing the contact angle develops the hydrophobicity feature at the same time decreases the wettability feature [54–58]. The various contact angle values are examined for PMMA (derived by the different expensive processes) in the literature [35–37]. The contact-angle measurement test has been applied in order to understand the develepment of hydrophobic or the hydrophilic surface at this study. The water drop was used as the liquid material for the contact angle measurement. This measurement provided information about the surface wettability property with the help of Attension Theta device in this study. Rockwell Hardness test was applied to determine the mechanical strength. The details about the results of XRD analysis, TGA/DSC, Raman analysis, SEM images, hardness and elastic parameters of the base PMMA and the PMMA/Borax hybrid composite samples were presented at 2 and 7.5 wt% borax amount in our previous study [40].

Methods for optical and density measurements

The transmittance T (%) (in Fig. 8) and reflectance R (%) (in Fig. 9) were measured between 280–1100 nm by using a UV–VIS spectrophotometer. The lightness value, L* of white was evaluated according to the CIELAB colour space (as the color model to explaine color differences) considering the CIE chromaticity diagram (as the projection of the three-dimensional colors onto the two-dimensional plane) to indicate green and cyan colour zones [26–28]. Quantachrome Autotap Density Analyzer was used with the automating the measurement process for measuring the density of powders.

Results and discussions

PMMA reinforced with borax decahydrate filler has been synthesized to make the development of hybrid poly (methyl methacrylate)/borax composite. The reinforcement has improved optical properties and enhanced amphibious behavior (for use in several applications such as optical devices, marine compatible materials, and biomedical materials). The physical characteristics of PMMA were modified with borax decahydrate addition (for its utilization in lightweight constructions at sea and terrestrial applications). The borax particle utilization at high amount (used extensively in industrial applications) has indicated the importance of the experimental investigations about the limit of the borax amount (at ~ 10 wt%) to avoid the clustering tendency of the borax micro particles in the PMMA derived by ATRP metmod. The use of a combination of methyl methacrylate (PMMA) and borax has created this polymer composite with unique optical features and mechanical properties. The ATRP method has provided some formations such as the carbon–carbon bond with a transition metal catalys to obtain the adaptable polymer and to modify the amphibious contions in this study. The borax component was thought to improve the hydrophilic nature of this polymer composite, while the PMMA component has provided stability and supported maintain the optical modification of this composite.

The development of the poly (methyl methacrylate)/borax hybrid composite (by using borax particles) enables modification of the structure to improve the communication enhancement of the system at several frequencies (such as X-band and Ka-band radar frequencies) [7, 24–38, 40, 59–72]. The results of this composite for the wireless communication system indicated that the wayfinding could be improved for withstanding natural disasters and saving lives by tackling global challenges by using the PMMA / Borax composite at contact with the ambient according to literature [7, 24–38, 40–43, 59–73].

The optimum shape and the crosslinked networks have been provided by using the polymer chains (grown in the controlled manner by the addition of monomers to this formation in ATRP method). The development of the functional device was performed by using the crosslinked PMMA/Borax composite based on ATRP method. The results of this composite indicated that the wayfinding could be improved by using the PMMA/Borax composite at the connection with other devices in the study environment. The crosslinked PMMA / Borax composite was synthesized by using ATRP method. The passive polymer was activated in this controlled polymerization method. The passive polymer has been functionalized by using CuBr initiator with the enhancement of this polymer composite with the improved molecular weight based on ATRP method. Borax addition has caused to the enhancement at the mechanical resistance to elastic deformation and shear deformation of PMMA/Borax composite [40]. The rise in the borax amount has provided resistance agains to compression and shear forces. The development of the mechanical performance about the resistance of the deformation and the return to its original shape at the polymer composite reinforced with borax. The

structure of PMMA/Borax composite has become more durable and rigid as the surface hardness increased [40].

The results of the bonding development of the composite in this study has indicated that the borax addition provided an increase of the deformation resistance in the composite structure. The results of this study have indicated the relation between the optical enhangecemet related with the density development of the PMMA/Borax composite and the improvement of anti-elastic resistance by borax addition. Rheological features of PMMA/Borax composite (such as elasticity, yield stress, and shear stress [40]) have indicated the critical details about the density development related due to the modification of the synthesis step and the optical development (as the result of the elimination of the mechanical deformation of this composite reinforced with borax). The use of this metal halide at the ATRP method has provided to form the active polymer radical based on copper due to the robustness and cost effectiveness. 3D images were taken from the surfaces of the samples to identify the elimination of agglomeration by using a stereo microscope in Fig. 2. Scanning Electron Microscope (SEM) analysis has provided to have information about the surface morphology to examine the effect of the rise of the borax amount on the surface roughness at the base PMMA (Fig. 3a), borax particles (Fig. 3b). Besides, SEM images have been presented such as the PMMA / Borax hybrid composites at 5% wt (in Fig. 3c) and 10% wt (in Fig. 3d) borax. The surface morphology of the composite indicated the uniform and homogeneous dissolution of borax particles (with the maximum size at ~ 50 µm) in PMMA. The use of the borax particles has provided avoiding the particle clustering (in the composite containing two different borax amounts). The base PMMA sample had more flat surface with free from any scratches. The surface has reached more grainy surface as the result of the increase of the amount of the borax in the composite. The superficial and randomly oriented flaws originating from grinding have been determined at 5 wt % borax reinforcement (Fig. 3c). The highest amount of borax addition (at 10 wt %) (in Fig. 3d) has indicated the tendency about the deeper cracks aligned at transverse direction with grinding in Fig. 3d. The increase in the borax amount resulted with the agglomeration tendency. The optimum homogenious dissolution of the particles occurred in the PMMA/Borax composite (including the borax at 10 wt %). The differences of the flow of borax micro particles in the polymer solution indicated the solution of the fundamental agglomeration issues at high borax amount in the polymerization. Hence it was avoid from the borax particle clustering tendency in PMMA and this study has explained the critical borax amount at 10 wt %. The images of the material cross-section have been added for base PMMA (in Fig. 3e) and the PMMA/Borax composite (at 5 wt.% borax amount) (in Fig. 3f) to identify the differences at the minimum borax amount and to complement the surface images. The cross-sectional images have indicated that the particles have been dissolved through the volume of the material homogeneously at the minimum borax amount.

The element identification by EDX has been confirmed by complementary analyses such as SEM and XRD analysis. EDX analysis has provided to identify the peaks indicated the sodium and boron peaks in the EDS pattern of PMMA/Borax (5 and 10 wt%) in Fig. 4. The similar peaks indicating the sodium and boron peaks are presented in the EDS pattern of borax at the literatüre [41]. The carbon, copper,

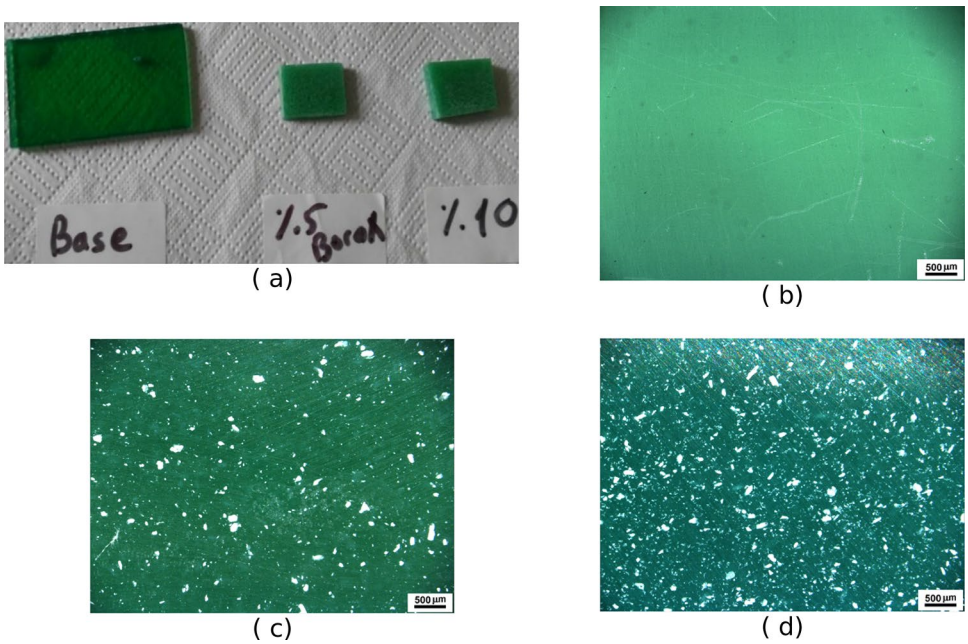

Fig. 2 Stereomicroscope images of base PMMA and 5, 10 wt.% PMMA/Borax

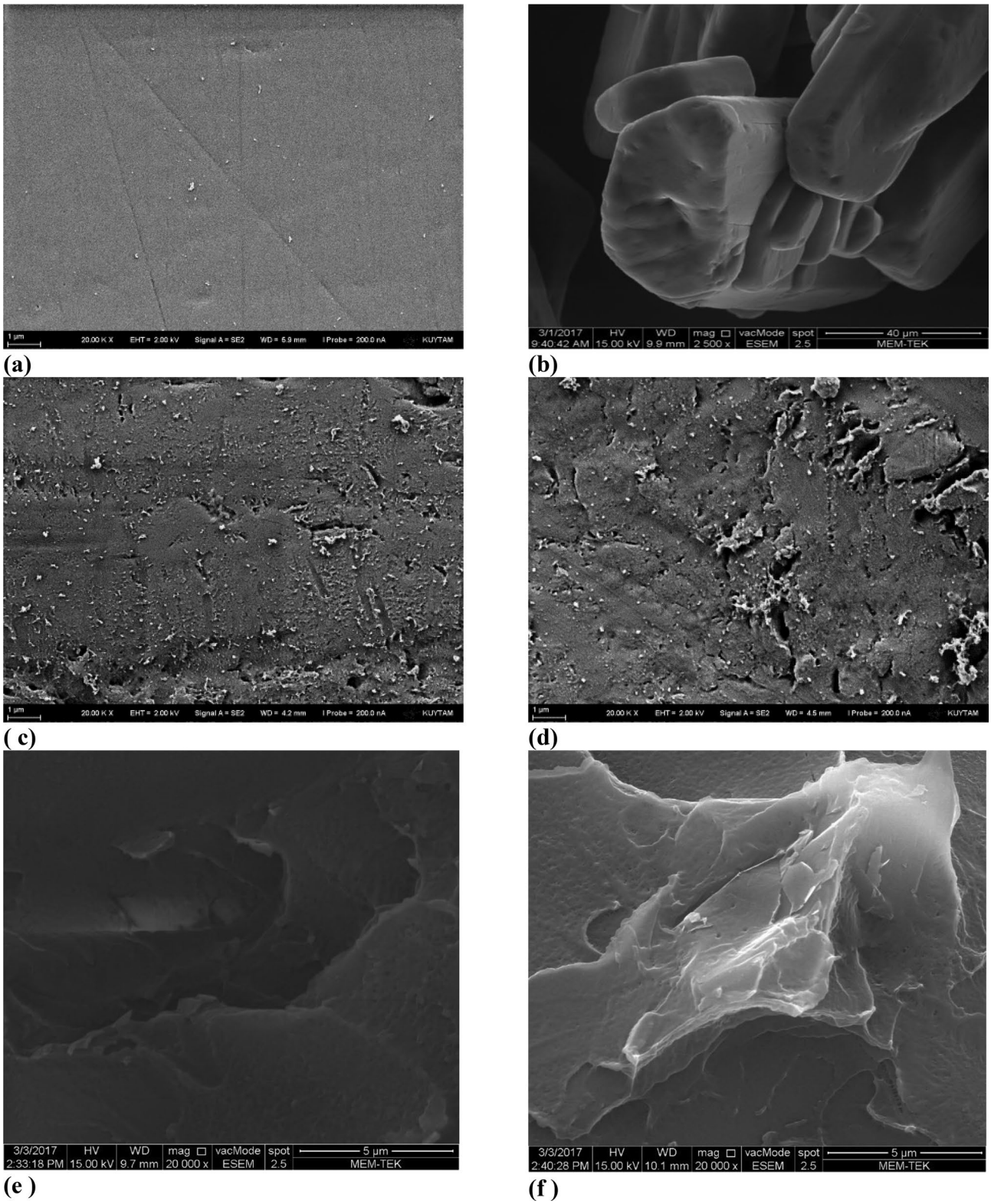

Fig. 3 Surface morphologies (in SEM images) for **a** PMMA, **b** Borax particles and PMMA/Borax at **c** 5 wt. % borax amount, **d** 10 wt. % borax amount, **e** the cross-sectional image of base PMMA, **f** the cross-sectional image of the PMMA/Borax composite (at 5 wt.% borax amount)

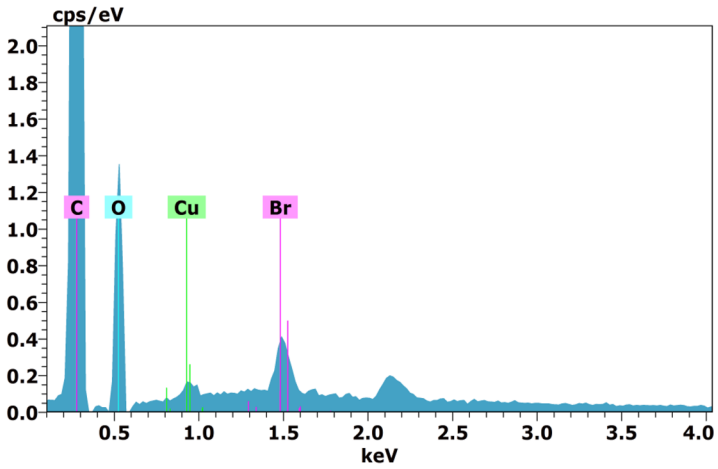

(a)

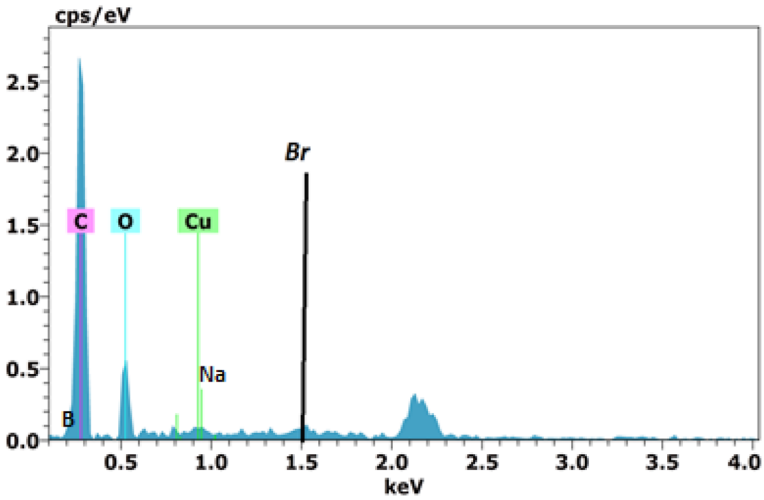

(b)

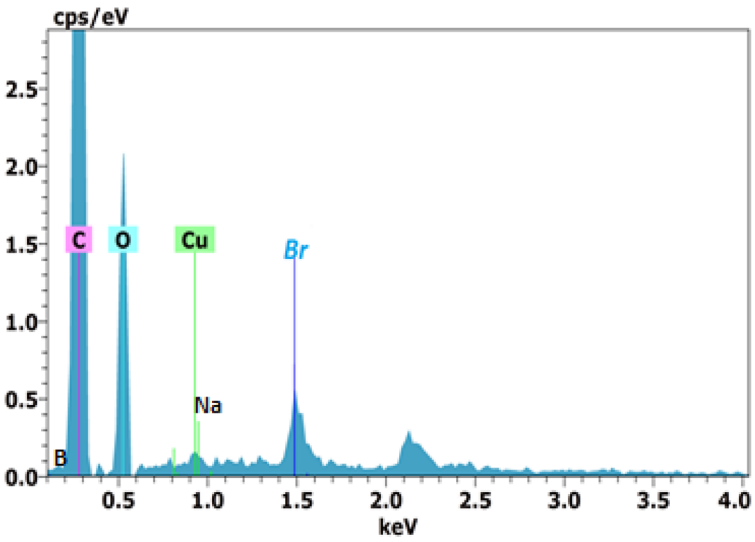

(c)

Fig. 4 EDX analysis of **a** PMMA specimen and PMMA/Borax specimen at **b** 5 wt. % borax amount, **c** 10 wt. % borax amount

oxygen, and bromine were determined at base PMMA in EDS analysis (Fig. 4a). The carbon atoms were identified coming from the used Bu_4NBr, PMDETA, EBIB in the synthesis. Bromine (in Bu_4NBr) was available in the composite. Bromide and copper atoms were at CuBr. The PMMA/Borax composite surface at 5 wt % (Fig. 4b) and the PMMA/Borax composite surface at 10 wt% (Fig. 4c) have presented the similar structure to the base PMMA. Boron peaks have been appeared at ~ 0.18 keV (boron Kα peaks), 0.2 keV (boron Kβ peaks) and. The low energy peaks of boron have appeared and accompanied with the presence of carbon (C) peaks at ~ 0.28 keV (carbon Kα peaks). The detection of boron (as a light element) was difficult to distinguish from other nearby peaks at low amounts. EDS analysis has indicated that the borox amounts (at 5 wt% and 10 wt%) were suitable to identy slightly the EDS peaks of boron. Na peaks have been appeared slightly at ~ 1.04 keV (sodium Kα) and 1.17 keV (sodium Kβ) in EDS patterns. The detection of sodium (as a light element) was difficult to distinguish in low concentrations. This study has indicated that the borox amounts (at 5 wt% and 10 wt%) at the PMMA synthesis were enought to quantify slightly the EDS peaks of sodium in the composite.

XRD analysis results have indicated borax at ~ 15, 18, 20, 25 and 30 (2theta degree) (Fig. 5). Similar XRD peak results are determined for PMMA/Borax composite [40] and borax particles [73]. Three broad prominent humps have been distinguished ~ 10°–25°, 25–35°, and 35–45° at the XRD curve of the PMMA. The similar peaks are informed in comparable polymeric structures [64, 65]. The intensity of the humps has been identified at the PMMA and the PMMA/Borax samples. Similar variations at base PMMA were determined in the composite. The humps of the peaks were available between 10°- 20°, 25°-35°, and at ~ 42° and these results were consistent with the peak values of borax decahydrate in XRD analysis [59]. A strong hump was formed at ~ 13° and a second hump was formed at ~ 30°. A small hump was available at ~ 42°. The hump value ~ 13° explanined the sequence and distribution at the PMMA chain. The hump values (formed at ~ 30°) have arisen due to the formation of Br-ions. Br-ions formed by CuBr (used as a catalyst in the ATRP method) and Bu_4NBr (used as solvent) caused the formation of this hump. Peak values were identified at 10.8°, 20.4°, 25.9°, 30.6°, and 40.7°. Crystallite sizes (calculated by using the Scherer equation in Eq. 1) have indicated a development derived from the peak values in Fig. 5. Their results were presented in Table 1. The average surface roughness increased slightly with the rise of the borax filler concentration in the composite. In the XRD analysis, the borax reinforcement effect at 5 wt.% has been distinguished slightly the XRD peaks.

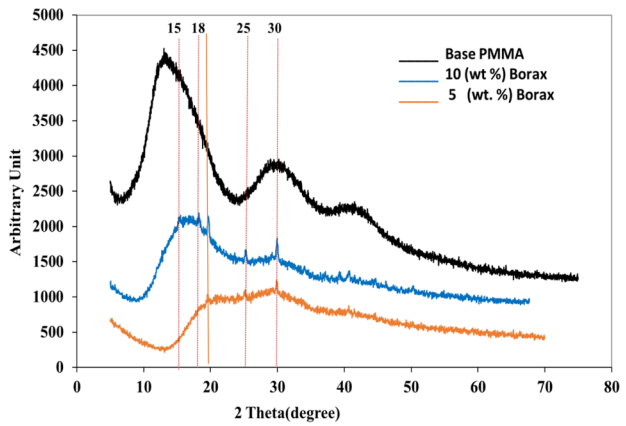

Fig. 5 XRD analysis of borax particles, base PMMA, PMMA/Borax composite

When sodium borohydride tetrahydrate ($NaB(OH)_4{\cdot}2H_2O$) (white crystalline solid used as the reducing agent) was mixed with copper bromide (CuBr) (used as the catalyst), the redox reaction was occured that resulted in the reduction of CuBr to copper metal (Cu) and the oxidation of $NaB(OH)_4{\cdot}2H_2O$ to sodium metaborate ($NaBO_2$) in Eq. 2. CuBr was oxidized, and $NaB(OH)_4{\cdot}2H_2O$ was reduced in the reaction (proceeding by the electrons transfer between two compounds). The interaction mechanism between $NaB(OH)_4{\cdot}2H_2O$ and CuBr has been controlled by using the reaction conditions (such as the temperature, solvent amount, and catalyst amount at the synthesis). $NaBO_2$ was used as the buffering agent to maintain the solubility and stability of the solution at the synthesis, and the mechanical efficency of the composite within the optimum range. $NaBO_2$ (as a type of the corrosion inhibitor named the passivator) was used to prevent corrosion and to form the protective layer at the composite preventing corrosion. The XRD diffraction pattern of $NaBO_2$ depending on the synthesis method, the size of its crystalline structure has presented the characteristic peak intensity and width of $NaBO_2$ crystal. The XRD diffraction pattern of $NaBO_2$ has exhibited the diffraction peaks at ~ 12.1, 20.3, 24.8, 30.1, and 36.8 degrees (2θ), which correspond to the (010), (001), (011), (002), and (121) crystallographic planes, respectively similar with the literature [44, 45].

$$2NaB(OH)_4 2H_2O + 3CuBr \rightarrow 3Cu + 2NaBO_2 + 8H_2O + 2HBr \quad (2)$$

The density improvement with the rise of the borax amount was examined clearly in Table 2. The density of the samples was determined by using the pycnometer to the assessment of specific gravity of the specimens. In order for the vehicle to remain in balance at the water under all climate conditions in the sea, the lifting point must be near the centre of gravity. The determination of the specific gravity of samples has helped in the calculation of the density values as the result of the rise in the borax amount in PMMA. The use of the synthesis technique of this composite (the density

Table 2 The changes of the density with the addition of borax in PMMA

PMMA/Borax Samples (wt.% borax)	Density (kg/m^3)
Base PMMA	1068
2	1094
5	1089
7.5	1124
10	1170

was similar to the density of water) has improved its use in extreme conditions. Because, the vehicle density must be similar to the density of water in order for the composite structure to float in water and to solve the capsizing problem (without the use of balloons etc. attached to the sides).

Gamma transmission was used to make an assessment of the density variation and the changes of the density of the composite was evaluated in Fig. 6. For this purpose, a certified Co-60 radioisotope was used as a gamma source. Lambert–Beer equation (according to $I = I_0\, e^{-(\mu . x)}$) has indicated the variation of the gamma ray attenuation of the composite with the rise of the density of the thermoplastic structure. I was the intensity of gamma ray passed through the composite with x thickness (mm). I_0 was the initial gamma ray intensity without the composite. The measurement of the transmission of the gamma radiation in the composite was replicated by five times in the experiments for the evaluation of the changes in the density. The transmission of the gamma radiation was evaluated by the relative intensity (I/I_0). μ was the linear attenuation coefficient which depended on the energy of the gamma photon of Co-60 radioisotope at 1.25 MeV. Gamma ray transmission was control with the decrease of the density with the increase of the borax amount in the PMMA structure. The gamma transmission technique (for 1.25 MeV gamma photons) has indicated the slight development of the gamma ray shielding performance for the composite at the minimum amount of the borax addiation (such as 5 wt. %). Linear attenuation coefficient of the composite was increased from 0,007 to 0,071 slightly by the addition of borax microparticles at the PMMA. The gamma transmission technique has supported to identify the change in density (in a minimum borax amount) at the base PMMA. The increase in the radiation attenuation coefficient has indicated an increase in the density of the PMMA structure by the borax addition at the minimum borax contribution. The borax (used as the filler microparticle) has provided the structural bonding development at PMMA (as a thermoplastic) as the rise of

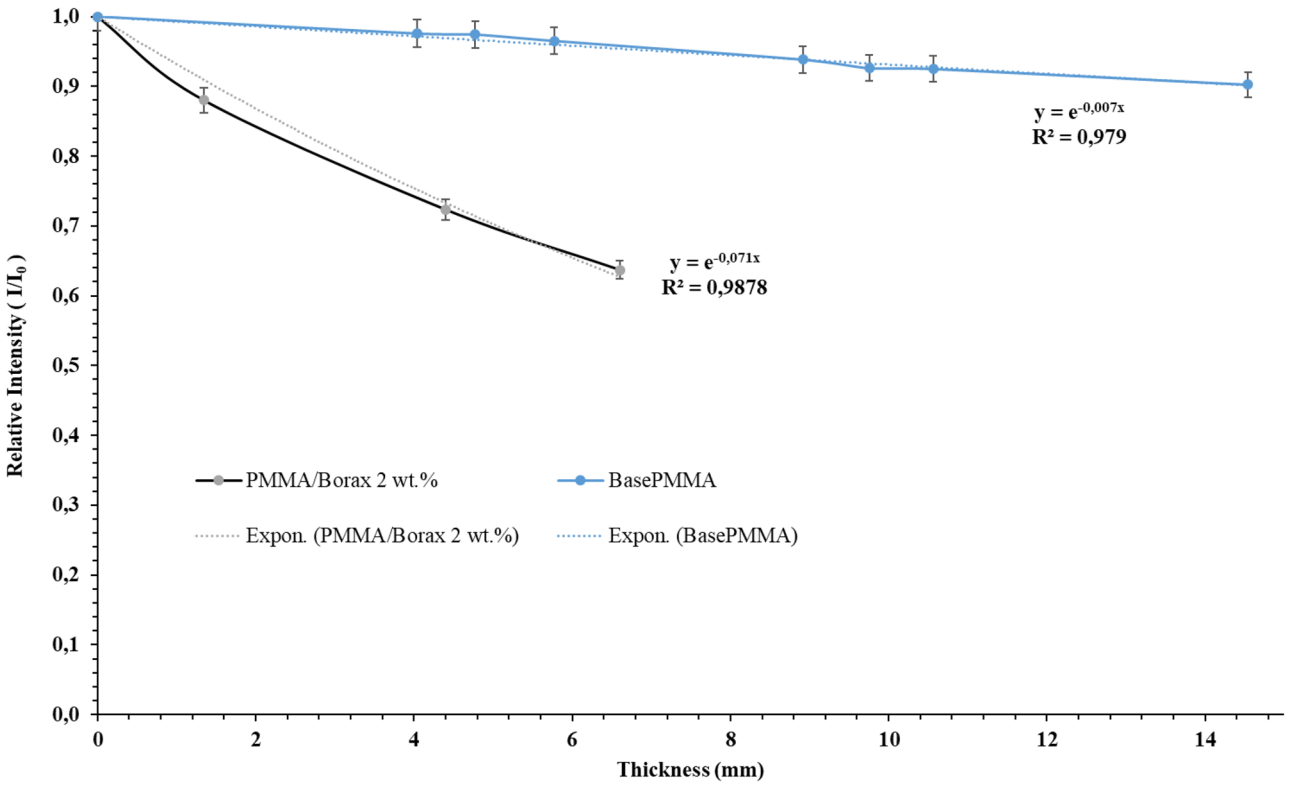

Fig. 6 The changes of the relative intensity of the gamma photons (emitted from Co-60 radiosotope) at PMMA with the addition of the borax microparticles

the crystallite size (in Table 1) and the improvement of the density (in Table 2) in PMMA/Borax.

FTIR Spectroscopy was applied to examine the bond structures at the samples (at different amounts of borax decahydrate). FTIR analysis has enabled the determination of the number of bonds in Fig. 7. FTIR analysis has provided several information about the bonds in the samples (in Fig. 7). Peak values were determined at wavenumbers of ~ 750, 810, 841, 985, 1144, 1240, 1435, 1722, and 2950 cm^{-1}, respectively. The wavenumber at 2950 cm^{-1} explained C-H with the asymmetric stretching vibration at CH_3. The wavenumber at 1722 cm^{-1} explained C = O with strong stretching vibration. The wavenumber in 1435 cm^{-1} indicated C—H with the bending and scissoring vibration, the wavenumber at 1240 cm^{-1} indicated C-O with the stretching vibration. The wavenumber at 1144 cm^{-1} explained C-H_2 with the bending vibration. The wavenumber at 985 cm^{-1} indicated BO_3 with the symmetric stretching vibration and 750 cm^{-1} explained C = O with the bending vibration. Although these bond properties are valid in all samples (5%, and 10% Borax/PMMA and base PMMA), another peak value at ~ 841 cm^{-1} wavelength was obtained for the sample containing 10% borax decahydrate and the base sample. The infra-red range between 4000–650 cm^{-1} was considered to identify the PMMA and PMMA reinforced with borax (in 5 and 10 wt % borax) in FTIR analysis. Their results were examined considering the wavenumbers of the peaks in Table 3a. The bonds (corresponding to the characteristic peaks) have indicated O–H bonds in the 3420 cm^{-1} determined at FTIR analysis for borax and PMMA/Borax and that the bond was derived partially as the result of the borax reinforcement at PMMA. The peaks have been derived in 2994 and 2952 cm^{-1} (belonging to the C—H with the stretching), 1772 cm^{-1} (for the C = O with the stretching), 1484 and 1435 cm^{-1} (for the C-H with the bending and scissoring), 1271 and 1240 cm^{-1} (for C-O with the stretching), 1190 cm^{-1} (for C – O—C with the bending) and 1144 cm^{-1} (for C—H_2 with the bending). A wavenumber has been derived in 1063 cm^{-1} (belonging to C-O with the stretching) at Table 3a. Table 3(b) has explained the importance of the reinforcement of PMMA with the borax particles. A wavenumber range (at 3600—3200 cm^{-1}) presented O–H with the stretching. This indicated the moisture at borax structure ($Na_2[B_4O_5(OH)_4]0.8H_2O$). The wavenumbers (with 1695 and 1650 cm^{-1}) indicated the H–O-H with the bending and the wavenumbers (at 1425 and 1360 cm^{-1})

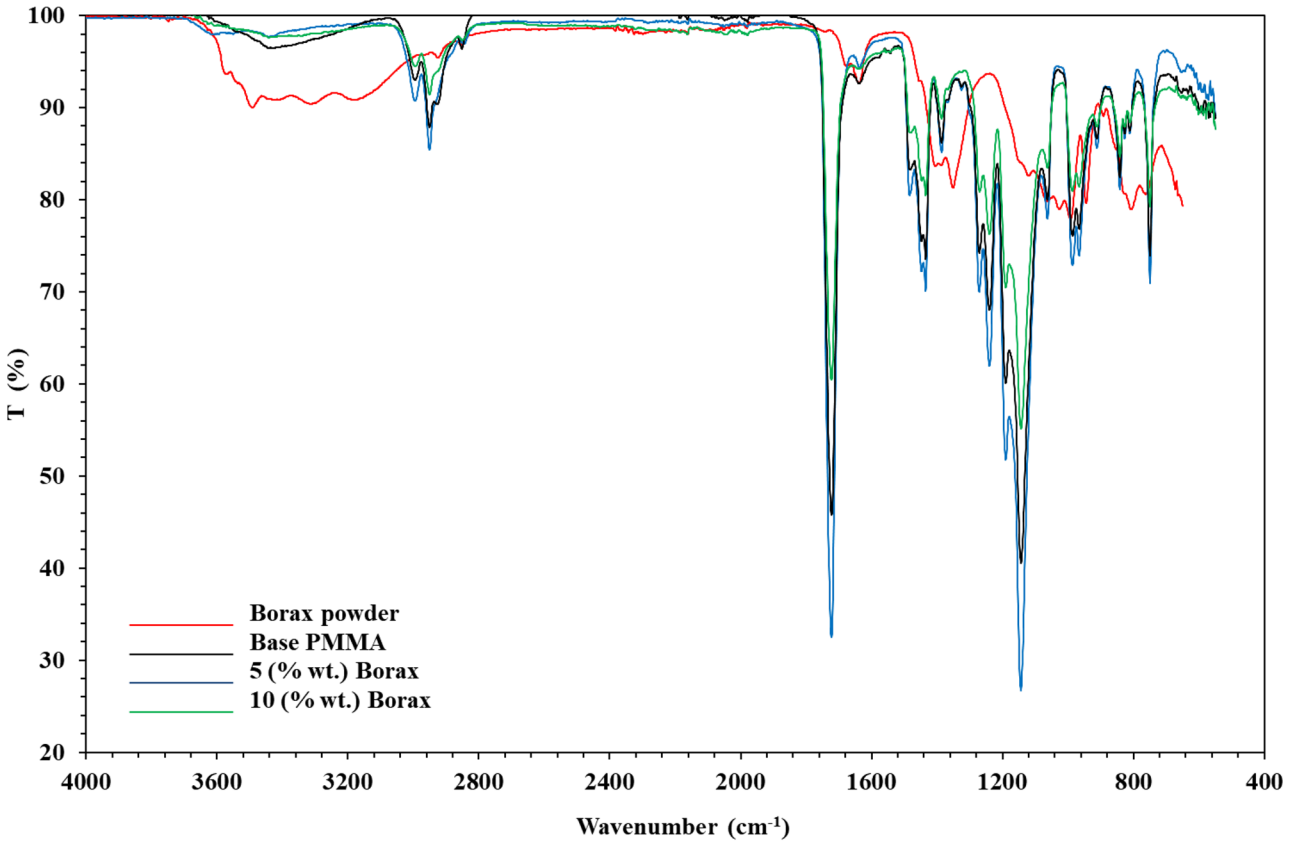

Fig. 7 FTIR spectroscopy result for borax, base PMMA and PMMA/Borax composite

Table 3 The developed bonds in (a) PMMA and PMMA/Borax (b) borax paticles

(a) Wavenumbers (cm^{-1})	Bond
3427	O–H stretching
2994	Csp^3H Stretching
2952	Csp^3H Strecthng
1722	C = O (Strong) Strecthing
1484–1435	C–H (with the bending and the scissoring)
1271	C-O (with the stretching)
1240	C-O (with the stretching)
1190	C–O–C (with the bending)
1144	$C-H_2$ (with the bending)
1063	C-O (with the stretching)
(b) Wavenumbers (cm^{-1})	Bond
3600–3200	O–H stretching
1695 and 1650	H-0-H bending
1425 and 1360	BO_3 asymmetric stretching
1161	B-0-H bending
1000 and 950	BO_3 symmetric stretching

explained BO_3 with the asymmetric stretching. The wavenumber in 1161 cm^{-1} has indicated the bonds such as B – O—H with bending. The wavenumbers (at 1000 and 950 cm^{-1}) explained BO_3 with the symmetric stretching. The details of the peak value at a wavenumber of 841 cm^{-1} is not available at literature [60–63] and the peak derived at this wavenumber has explained C-H with rocking vibration. It was assumed that it has emerged due to the strong C-H bonds derived by adding borax decahydrate to the PMMA structure. The wavenumber at 812 cm^{-1} indicated B-O–H with bending vibration, and this vibration indicated the bonds of boron atoms added to the PMMA chain with the addition of borax.

The contact angle values give significant amphibious properties of the PMMA [54, 55, 64–67]. The use of polymers (such as PMMA [7, 68–72] and other innovative polymers [24–38, 40]) in aggressive environments can be possible with the modification of the structural properties. The variations in contact angle measurement values were determined in Table 4. For the examination of static contact-angle, the variations were determined (for the contact angle was referring to the angle formed the based on the adhesive force) between water droplet and the surface of the sample. Their contact angle results were presented in Table 4. The base PMMA (with contact angle in ~ 95°) had hydrophobic feature. The borax addition in PMMAs has provided a hydrophilic feature (at ~ 81° for the sample with 5 wt % borax and at ~ 71° for the sample at 10 wt % borax amount). Methyl methacrylate (MMA) has been utilized as a monomer (which is smaller molecules). The MMA solubility is preffered as 15 g/l in 20 °C and a solubility at sodium tetraborate decahydrate at water is 38.1 g/l in 20 °C [56]. The surface of the samples (reinforced with borax) held more liquid. The contact angle measurement was carried out to determine the water-holding capacity at the surfaces, to determine the wettability properties, and to understand the hydrophilicity-hydrophobicity characteristics. The borax filler has developed hydrophilic properties in PMMA at this study. The measurement of the contact angle at the PMMA/Borax composites indicated borax reinforcement at PMMA. Borax reinforcement caused a decrease at the hydrophilic features. These results presented that PMMA had reached more hydrophilic structure with the addition of borax and it has indicated that contact angle values decreased. The increase in the amount of borax is determined to make an optimization at the thermal resistance and mass loss considering mechanical strength and the improvement of the bulk modulus values of PMMA/Borax composites (with the increase of the borax amount) is performed with optimum thermal performance (with the improvement of resistance of this polymer to the compression force) [40]. The results related to mechanical properties of PMMA/Borax composite is presented in the previous study [40]. Poisson Ratio, Young, Shear and Bulk Modulus and Microhardness are considered by using the ultrasound testing method based on the calculations of velocities of the transverse and longitudinal sound waves passing through the PMMA/Borax composite samples [40].

Shore-D hardness test indicated that hardness of PMMA (at 80,6) increases to the hardness value (at 86,2) with the addition of borax (at 5 wt.% amount) in PMMA. The addition of the borax microparticles has provided optimum flexibility in the PMMA matrix. The synthesized composite structure was controlled quickly and non-destructively by performing

Table 4 Contact-angle in PMMA and PMMA/Borax specimens with 5 and 10 wt % borax

Sample	Contact Angle Degree (°)	Contact-Angle Image
PMMA	~95	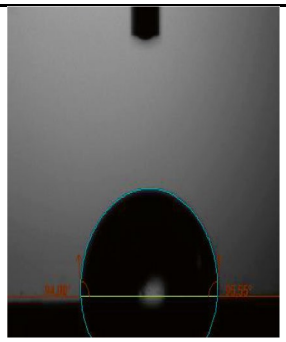
PMMA reinforced with borax (at 5 wt %)	~ 81	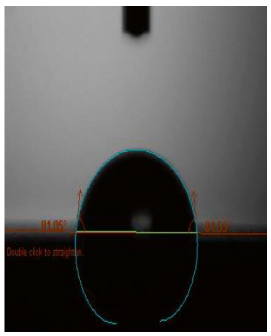
PMMA reinforced with borax (at 10 wt %)	~71	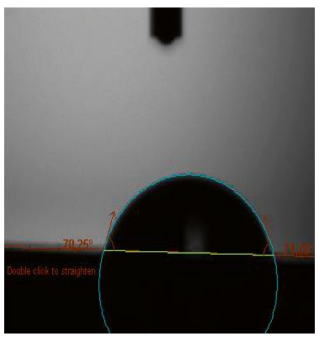

the hardness test in this study. The development of hardness indicated the improvement in the mechanical strength of the composite. When the surface hardness of PMMA/Borax composite was improved, the anti-elastic resistance could be increased. The development of the PMMA with the microsized borax particles addition has provided suitable reinforcement about the importance of mechanical property of composite. The results of the hardness test have indicated that the borax particles have been integrated well in the PMMA structure in order to improve the resistance of the composite structure against scratching, cutting, abrasion and puncture. PMMA solution provided to wrap the boron microparticles well and borax microparticles (added to the PMMA) was suitable for the improvement of the resistance of the composite structure against plastic deformation. The increase in roughness with the rise of the borax-decahydrate particle amount (in Figs. 2–3) has affected the wettability on the surfaces of the composite. It has changed the structural features slightly from hydrophobic to hydrophilic determined with the control of the contact angle. The transmittance T (%) (in Fig. 8) and reflectance R (%) (in Fig. 9) have presented the optical changes between 280–1100 nm. The optical features have been investigated at 2 mm thickness for all specimens. The increase in borax concentration has caused a decrease in optical transmittance (in a range between ~ 400–1100 nm) at the PMMA/Borax sample. The change in T (%) has indicated the enhancement of the amphibian biocolour as the result of the opaque feature of the specimen. The optical transmittance of base PMMA has presented a cut-off value beyond ~ 300 nm and T (%) has reached ~ 80% in a wavelength range (~ 360–380 nm). T (%) of this sample has reached 58% in ~ 550 nm (at maximum eye sensitivity of humans). The transmittance of the light photons slightly was in a range between 350–400 nm with the borax

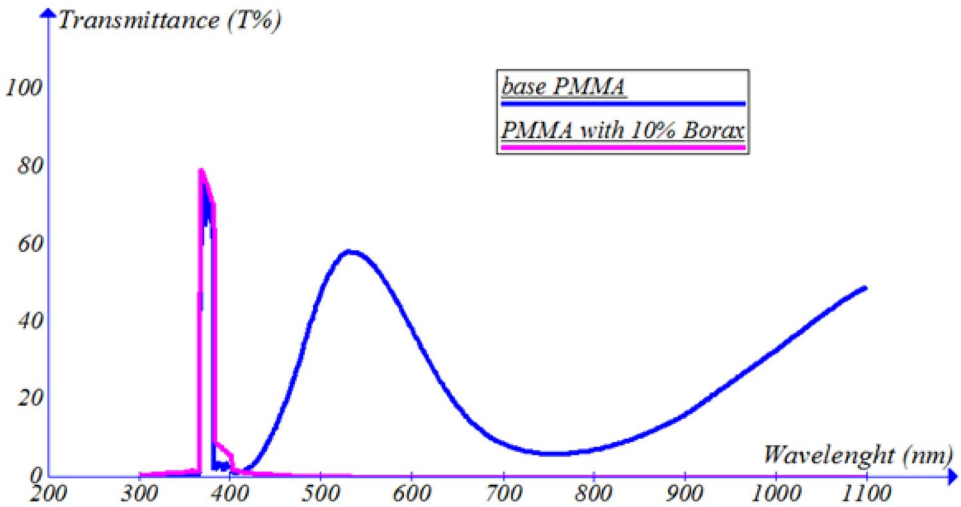

Fig. 8 Optical transmittance of the samples

addition. PMMA/Borax specimens (with borax addition at 10 wt %) have indicated a cut-off value beyond ~ 310 nm and T (%) decreased dramatically to 2 (%) at ~ 400 nm. The optical feature has changed from translucent to opaque at the sample reinforced with borax at 10 wt (%) (in Fig. 8).

R(%) of PMMA (in Fig. 9) has indicated that the scattering effect of light photons increased from both the grain boundies and the grains with the rise of borax concentration at the composite. The PMMA reinforcement (by using borax particles) has resulted in an increase in the reflectance R (%) slightly. R (%) of PMMA/Borax composite was determined between 300–1100 nm for PMMA and the PMMA/Borax specimens (with 5 and 10 wt % borax) in Fig. 9. R (%) has been developed in 380 nm wavelength and the reflected light intensity was at ~ 94% for all samples. R (%) decreased to 3% at the base PMMA in a wavelength range (550–1100 nm). R (%) of PMMA decreased dramatically as a result of the borax reinforcement. R (%) has reached 1 (%) at a critical borax amount (in 10 wt % borax). The absorption edge has presented the modification on light absorbance A (%) with the borax addition as the result of the blueshift indicating the change of the scattered light wavelength. The absorption edge has changed from 300 (at the base sample) to 310 nm (at the sample with 10 wt % borax). The borax reinforcement has developed the blocking light from travelling through the composite derived by using the ATRP method. The monomers (which are smaller molecules) are chemically combined to create larger molecules at polymerization step.

The variations of the optical transmittance and reflectance of PMMA (reinforced with borax) have provided an assessment of the optical absorbance (A% = 100-(T% + R%) with the variation of the absorption intensity of light photons at the

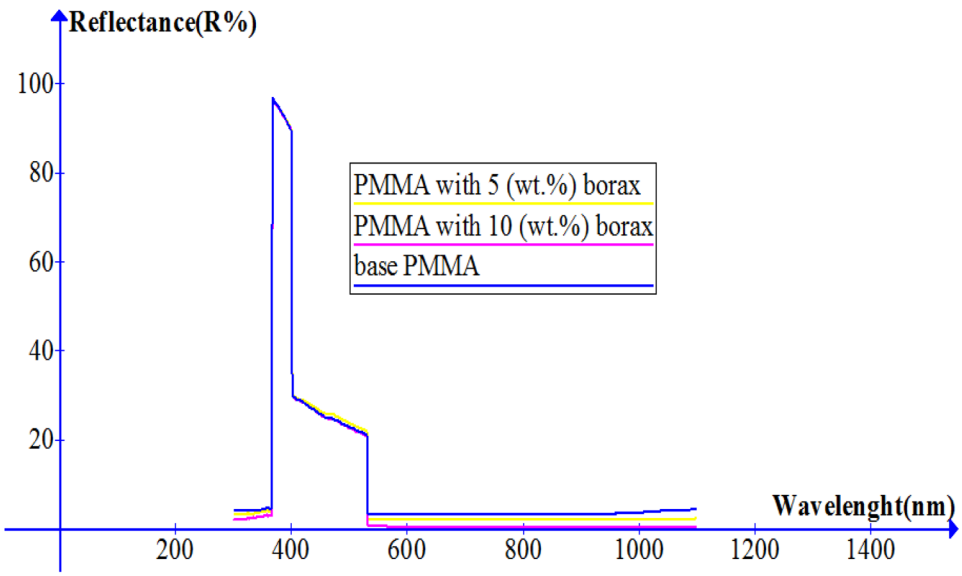

Fig. 9 Optical reflectance of the samples

PMMA) with the borax microparticles. A(%) of the samples rose considerably between 280—380 nm in the UV range and A (%) decreased over 380 nm with the development of new optical properties with the enhanced light transmittance and reflection (was considered novel). The lightness value, L* of white (at 100) defines white colour at the powdered borax with 91.92 L value according to the CIELAB colour space (considering CIE chromaticity diagram which indicates green and cyan colour zones) [26–28]. The multiple scattering effects of light photons have been efficient in the PMMA/Borax composite as the use of this hybrid polymer composite (in previously unexplored applications), such as in underwater optical devices or marine coatings, could also be considered novel. The self-absorption at the composite resulted in the decrease of absorption between 550–1100 nm due to the rise of borax amount at PMMA. The borax reinforcement has changed the optical behaviour of the light photons at the PMMA sample and the sample has reached more opaque features. The blueshift has indicated a decrease of the scattered light wavelength (with an increase in its energy) considering the energy conversion at the composite. The blueshift has presented the advantage to derive new features at the PMMA/Borax composite as cyan color of this polymer at the wavelenght absorbed fewer light photons than other color (such as green) materials in the electromagnetic spectrum. The PMMA/Borax specimens have increased the scattering of the light photons slightly at the wavelength of cyan colour due to the change of the colour of the composite. The improved cyan color (by the borax addition in PMMA) in this composite could allow light to penetrate deeper (such as into the water) as the result of a decrease in the dominant wavelength from 525 to 500 nm. The cyan colour of this composite has supported the scattering of the visible light photons as the result of the borax addition. The developed cyan color of this composite could support visual quality of the underwater environment as the light photons at the cyan colour wavelegth has travelled more energetically. The obvious biocolour was obtained dominantly by the absorption and the scattering of light photons from the grain boundies and the grains with the rise of borax amount (like the reemission of light from the living organisms with that amphibious biocolour having proteins which can be built into their skin or other tissues) [7, 24, 27, 29, 30]. The developed surface features have provided its distinguish in the marine environment. The addition of borax in PMMA has developed the composite to distinguish more clearly from far away.

The optical transmittance of base PMMA (with yellow line in Fig. 8) was performed at the green zone and its dominant wavelength was centered at ~ 525 nm in the CIE chromaticity diagram. The transmittance of the PMMA/Borax composite decreased at 10 wt % between 410 and 1100 nm. As the composite colour has shifted slightly from green colour zone to cyan colour zone in the CIE chromaticity diagram, the light photons at the cyan colour wavelength has presented the higher penetration depth than green colour wavelength (such as, in water) for use in the specific amphibious colour technologies. The dominant wavelength shifted to ~ 500 nm providing more control of amphibious colour in the PMMA/Borax sample with 10 wt % borax (that could be suitable for the use of this composite in underwater lighting and development of the photography equipments). The advantage of the shifting of the dominant wavelength (from 525 to 500 nm) has been provided to distinguish this sample (with 10 wt % borax) more clearly from far away depending on the rise of the borax amount in denser media (such as aqua) than air. As the development of the cyan colour (providing highly visible color in water) has support to distinguish more clearly this composite at the greater depths, this colour could enhance the appearance of the composite for several tactical applications (such as, for the location of the systems including cyan colour at marine life and the finding of the target in underwater scenery). As the cyan colour provide more visible quality in specific environment it could provide the ability to higher visibility (such as, in underwater). Figure 10 showed the map of the chromaticity coordinates (x, y) of the emitted light in the CIE chromaticity diagram.

The PMMA/Borax composite scattered the cyan colour known as the color of shallow tropical waters and had several advantages of cyan color in shallow tropical waters and sea. As the cyan colour of PMMA/Borax composite supported the dominant wavelength shifted to ~ 500 nm, cyan colour supported camouflage in water by providing

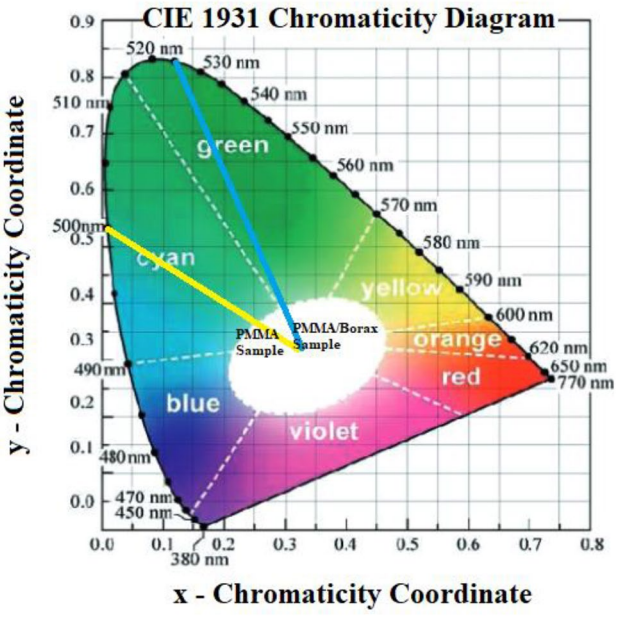

Fig. 10 The chromaticity coordinates of the PMMA based sample and the PMMA/Borax composite decreased in 10 wt % sample at CIE (1931) chromaticity diagram

a background color. The cyan color of PMMA/Borax composite had the key parameter in aquatic camouflage, supporting to protect and conceal the system in the water. The appropriate color selection based on the specific requirements with the addition of borax (10 wt %) has provided to avoid detection and to sneak up on target. The cyan colour of the composite has supported camouflage of the system with their surroundings at underwater environment. The cyan color of the PMMA/Borax composite could help blend in with the coloration of rocks, coral, and other underwater structures (making them less visible to other systems) as the chromaticity coordinates of the light photons scattered from this composite due to the appropriate color selection (as cyan colour). In this study, the transition metal catalyst including copper atoms (which has given green colour to the composite) was important due to its performance at the ATRP method to enhance the optical feature of the PMMA with green colour (which can absorb energy from sunlight considerably and scattered it at lower energy wavelengths as a different color in living organisms) in a decrease of the dominant wavelength (from 525 to 500 nm). It was assumed that the photons in the visible range collided more effectively at the grain boundaries and the grains. The photons scattered dominantly at the rough surface when the borax amount increased in PMMA. The scattering continued until the photon was left from the surface. The photon in the visible range moved outward from the surface. The effectiveness of cyan colour was important as a camouflage colour depending on the specific environment. The photon in the visible range increased and travelled with high energy as its energy increased. As the scattered photon's energy increased, it resulted in more difficult detectable visible light. The photon energy decreased slightly after each collision on the surface.

The decrease of the dominant light wavelength of this composite has indicated the variation of the colour shade perceived by the human eye. The results of the contact angle measurements and the surface images (at SEM analysis and the Stereomicroscope) have indicated the reason of the increase in wettability. The slight tendency of the agglomeration has occurred with the rise in the borax amount. The increase in borax amount caused a slight decrease in the contact angle value of the surface. A more hydrophilic surface has been formed when the samples transferred to the marine ambient. As the control of the surface feature was provided without the use of the extra layer of oxygen, this single layer has been supported to protect the electronic configuration practically and to produce a useful configuration for the development of the aquatic surface at the composite. The amphibious system based on the PMMA/Borax hybrid composite has been synthesized to obtain a new industrial development for its futuristic design (with the amphibious features). The amphibious features were developed to protect the equipments effectively in corrosive ambient when using this amphibious polymer (such as, for the delivery).

The amphibious green colour of samples was provided by using copper which comes from the used catalyst (CuBr) at the synthesis. Experimental data for the development of the PMMA/Borax composite has provided a physical understanding of the dissolution phenomenon about the borax micro particles at the PMMA in this study. The chemical composition of this composite has included a certain amount borax to obtain a suitable harmony in the design including optimum geometric shapes on the surface for clear harmony between the composite surface and aquatic ambient. The composite appeared with green colour dominantly by using the ATRP method with the presence of the CuBr metal halide (involving the chain initiation of free radical polymerization by using EBIB and the result of the initiator triggered chemical reaction). This chemical method (providing in situ polymerization with the mixing of chemicals in the monomer) has allowed the living polymerization to improve the scattering of light by the addition of borax micro particles at the composite structure presenting the optimum biocolour. The samples (with the clear harmony between the composite surface and aquatic ambient) have absorbed the wavelength mainly centred blue and red light in the electromagnetic spectrum. As the borax in PMMA has provided to modify the composite's optical properties in novel ways the samples have reflected green light in a spesific colour tone. The synthesized green composite samples have provided to lead more predictable and controllable photon scattering properties and absorbed sunlight effectively. The main challenge involved in colour generation (as the control of chemical composition in the composites) has provided to modify the composite's surface properties and enhance its photon scattering ability. The novel impact of the synthesis of the composite has developed the applications for photon scattering (to make the bridge the gap between the structural features and amphibion biocolour) at the implications for a wide range of fields, from optics and photonics to biotechnology and energy. The designed surface morphology (formed with addition of borax) with visually amphibious green colour harmony has supported to make the satisfying distinguish effect from far away with the combination of the used elements. The development of the distinction of the hybrid poly (methyl methacrylate)/borax composite for the use in service area has been obtained in the critical borax amount at 10 wt % as the result of the optimum chemical composition of this functional polymer composite.

The composite was synthesized to obtain an alternative lightweight and durable materials for use with the variety of underwater applications (such as boat hulls, buoys, and diving gear). The properties of this hybrid polymer were developed for new products and technologies with its improved performance and functionality of amphibious vehicles

(designing to travel on land and water). The relation between the rise of the borax decahydrate amount and the generation of the optical feature has been determined (with the modified hydrophilic feature) to improve its surface quality. The properties of this composite have been modified to solve its integration problems in its amphibious applications which could result in protection of the surface against dusty or oily areas. The results of this study indicated that the preparation of this composites with optimum amount borax (used as lightweight filler) could be significant for the effective physical features of the composite (such as for use at the oil and gas exploitation systems in the seabed).

The back-and-forth thrust power is created at the ships due to the wave conditions in the sea. The action-reaction motion principle created by this movement affects the vehicle's right-left turning and sliding. It is important that the vehicle at "rest" rotates around its own axis one full turn and is stable at the sea. As it is difficult for the system to capsize in dead water, the torque effect of the system is practically sufficient to straighten the system itself. Hence it is practical that the centre of gravity of the vehicle can be kept at the optimum place and air entry into the composite can be prevented. Therefore, when the vehicle rolls over, it returns easily to a level position, as it should. When the vehicle is on duty in rough seas, it should maintain this capability. If the sea has huge rough waves, the amphibious vehicle becomes more problematic. The required polymer (improved molecular mass by ATRP polymerization) will more easily turn itself around without harming the crew inside in case of capsizing. It was assumed that the modification of the density has supported that the hybrid structure (which could be able to fill a needed gap in amphibious systems) was built for use in the sea (in Table 2). Because the direction (in which the water exerts force) can change momentarily at a moment in the rough sea when the wave rises—falls. In such a case, the system can be self-accelerated so that the vehicle rolls in the water. This can be considered a negligible test condition or probability. Because the vehicle could not stand upside down for a long time in the water and tends to correct itself with a small change of centre of gravity.

The entire load could not be placed on one side in maritime trade as the vehicle cannot go very far if disaster strikes at sea. The vehicle must be able to move parallel to the ground in order to create a turning/upsetting moment when necessary. It is important to achieve this in the fully loaded test with the personnel not wearing the seat belt inside. When the weights of the personnel are added where they should be placed, it is important that the polymer stays above the water in this order. As the direction of the centre of gravity always moves down changing the centre of gravity can cause the vehicle to capsize in the rough sea. For this reason, the equipment and personnel are loaded evenly while loading the vehicle. If the ship hits the waves at sea, it slows the ship down by changing the speed of the ship and by changing the heading of the ship. Hence, it is important to design the vehicle with the edge lines of the vehicle as completely horizontal or at an angle of a maximum of 45 degrees (instead of being vertical and at right angles) to reduce the pressure effect of the equipment on the vehicle. Smaller and thinner vehicles are preferred against waves, and they can be synthesized from thermoplastics to derive as horizontal or at an angle of a maximum of 45 degrees. Thin edges (synthesized sensitively by the ATRP method) could be beneficial against huge rough waves so that the ship does not turn its head (bow) at the hill of the huge waves in the rough sea. As the modification of the thin edges, the synthesis of the PMMA/Borax composite (such as the thermoplastic polymer) derived from the ATRP method that could not cause problems in storms and the establishment of the full balance could be important depending on the weather conditions.

The gravitational water influence has provided to eliminate slightly the gravity effect of water on the surface. There were two important parameters to modify the surface of lightweight PMMA with the borax addition depending on the hydrophilic surface with the development of amphibious featues such as improved buoyancy. The hydrophilic properties of polymer composites formed by adding borax to PMMA polymer (as the amphiphilic polymers) increased and their wettability feature has been increased. Micro-sized borax particles have influenced the wettability and the surface roughness of the composite (in Table 4–5). Borax microparticles have had the key role influencing the modification of the hydrophobic surface. The wettability feature was developed with the modification of the water holding capacity on the surface of this amphibious green colour composite. The based-PMMA derived by ATRP method has had hydrophobic features at 95° contact angle value and this contact angle (Table 5) was higher than literature [31–34]. This contact angle in this study has resulted in less wetting. It can be used outdoors at the rainy weather. The contact angle value causes slight increase. The sample surface has holded less water while the sample has been utilized at outdoors. The slight increase could support saving fuel as this material is used in several technological areas (such as transportation technologies etc.). The contact angle value in PMMA reinforced with borax (in 5 wt.%) has had 81° value. The contact angle value at PMMA (improved with the borax addition at 10 wt.% amount) was determined as 71° at this study. The reinforcement with borax resulted with the decrease at contact angle in the surface of the polymer. But the results of this study has indicated the original results that the hydrophobic features in base PMMA derived by ATRP method was turned into hydrophilic features gradually as the rise of the borax amount. The borax reinforcement of PMMA caused the generation of hydrophilic self-cleaning feature at the surface (which could reduce the dirt and contaminants

Table 5 Contact angle values of PMMA at this study and literature [31–34]

Polymer	Fabrication of polymer	Contact Angle Value (°)
PMMA [31]	Purchased from Industrial Insulation Chennai Company at India (PDI = 1.82) Mw = 93.9 kg/mole	~ 73
PMMA [32]	Purchased from Industrial Insulation Chennai, India	~ 60–70
PMMA [33]	Free radical synthesis by Sigma Aldrich	64
PMMA [34]	Homopolymer (Mn 90 kg/mole), PDI = 1.09	69
Polyester sample with 1.5% borax [43]	Polyesters blended with borax mineral	72,77
base PMMA (in this study)	ATRP Method (Mw = 270 kg/mole)	~ 95
PMMA at 5 (wt.%) borax (in this study)	ATRP Method (Mw = 275 kg/mole)	~ 81
PMMA at 10 (wt.%) borax (in this study)	ATRP Method (Mw = 670 kg/mole)	~ 71

as the result of the dissolution of smaller particles) when the water drop was contacted to the composite surface). The modification of its hydrophilic surface provided the self-cleaning feature at the specimens. This modification at amphibious features has indicated its potential applications (with the optimum treatment by the addition of borax microparticles at the composite) in corrosive ambient (such as sea water, salty water, blood etc.). The results of this study indicated the futuristic utilization of this composite that the roughness and wettability of this modified composite were the critical factors (for example in the cell colonization) for the specific applications (such as bone implantation in human body at the oncological treatments etc.).

The development of the roughness has indicated that this composite could be important for the bone incorporation of the composite as the result of the successful generation of surface roughness with the borax reinforcement (used at implant which could be improved the bone-implant interface). Besides, the development of the amphibious feature at the PMMA/Borax composite has presented a possibility of generation in small robotic amphibious vehicles (like the special living machines without employing a living cell). The atom transfer radical polymerization (ATRP) technique has provided the genenration of the living polymerization by using radical chains (like the inspired by animals at the biomimetic concept to navigate underwater and rough terrains and like the devices based on the several polymer systems called proteins in modern biology [29, 30]). The radical chains (which could be accepted like the vertebra of the living machines) have continued to grow by adding monomers to the radical mechanism in this study. As the PMMA/Borax composite structure has been produced by the ATRP method (like the living factory manner) and the structure could be capable of organizing itself, the whole polymer composite structure has been accepted as a smart machine in this study. As the propagating chain end has maintained its reactivity (like the increase of the vertebra numbers in the living small robots) it could be possible to make an assumption the evaluation about “to learn about living things and to study them while they are still alive". It was assumed that this living robot mechanism has been divided into backbones with the addition of borax in PMMA. It was assumed that this living robot mechanism could form a smart formation in which light created the activity in the PMMA/Borax composite to distinguish the composite more clearly from far away. The living polymer composite mechanism has been improved with the creation of the diversity of polymer links by using the ATRP method. This mechanism has been more complicated (like "in vivo") as the result of the reinforcement of the diversity of polymer links with the connection of the developed grains by the addition of the borax microparticles in PMMA. The rise of the propagating chains (like the simple pieces of living nature in the lab) has increased the mechanical performance of this polymer (called living polymer [20]). The propagating chain has recaptured radical chains before they had a chance to undergo the chain termination events (like "in vitro"). The first ones of the radical chains (which is the strongest) could function the impact requirements of new interior head specified as the brain of the living robot mechanism with the designed surface morphology (with addition of borax).

The development of a remotely (actuated amphibious) robot control with visually amphibious green colour harmony has indicated to use in futuristic studies on-terrestrial and inwater applications. The shifting of the dominant wavelength (from 525 to 500 nm) has revealed the futuristic potential applications of this composite in several parts of the robot mechanizm. The capabilities of the

novelty function could enable the development of the robot (including this composite) with the satisfying distinguish effect from far away. The combination of the used elements (with the optimum chemical composition of this functional polymer composite) could be suitable at the critical borax amount (for example its use as a potential minimally invasive devices by using borax microparticles at 10 wt. %) in good agreement at the experiment results. It was assumed that the increased surface roughness by using the borax cleaning agent could induce bone-composite interaction as the result of the increase of bone-antimicrobial implant (or the contact of this robotic mechanizm in complex environments such as the gastrointestinal tract). The chemical composition with the transition metal catalyst (including copper atoms which has given the novel green colour to the composite fabricated simply by ATRP method) was important at a certain amount borax to obtain a suitable design at the surface. The assesment of the crystalline size in polymer structures was performed effectively by Scherer Formula (in Eq. 1) [38]. It was possible to use the polymers in different areas (such as industrial and healthcare applications) with the optimum geometric shapes which induced the photon scattering abilities from the surface of hybrid poly (methyl methacrylate)/borax composite. The control of the dissolution of the borax microparticles in the PMMA matrix has supported to generate a more uniform surface with the enhanced optical property as the result of the modification of the crysttaline features of the composite. For the development of new applications with the composite's photon scattering properties (such as in optical sensors, displays, or lighting) the modified surface with polycrstallines has the optimum capability to absorbed suitable energy from sunlight. The modified geometric shapes on the surface has provided suitable scattering by the photons in visible range as the result of the development of new manufacturing technique of this composite.

Conclusion

The conclusion remarks have been presented considering the experimental results for this hybrid material. The development of optical features at PMMA/Borax samples (derived by using ATRP method) has modified the amphibious properties. The commented results of this functional polymer were summarized as follows:

1. The development of the structural bonding (by using borax filler) has presented the relationship between the rise of the crystallite size (resulting in a slight improvement of the density) and the density in PMMA/Borax.
2. PMMA/Borax sample (containing a certain amount of borax) has been quantitatively investigated (by using the reflectance and the transmittance values) for the evaluation of visible light scattering. The absorption edge has acted as the characteristic parameter in addition to the scattering. This lightweight density material had the strong dependency on light absorbance with the borax addition. The photon scattering has affected slightly to determine the change of absorption edge and the absorption edge has controlled by using the borax amount in the composite. The higher amount of borax, the higher the absorption probability was gradually between 280–1100 nm.
3. The PMMA/Borax composite has been enhanced and the amphibious green colour was supported to develop its distinguish more easily from far away depending on the rise of the borax amount.
4. The contact angle measurement results of PMMA/Borax decahydrate composite has indicated the slight modification of its amphibious properties with more hydrophilic surface. The development of the hydrophilic properties enhanced the width of the deflection of photons with the increase of the crystalline size due to the rise of borax amount (causing the development of the reflectance). When the borax decahydrate concentration reached 10 wt. %, the composite surface has resulted in the optimum rise of the wettability feature for the suitable objective in crystalline parameters and optical performance. The contact angle measurement results demonstrated that the hydrophilic surface in the PMMA/Borax decahydrate composite did not only serve to augment slightly the deflection of light (between 280–1100 nm) but also diminished its misclassification probabilities. The modified hydrophilic surface has reduced the classification uncertainty apart from an improved detection performance.

Acknowledgements This work was supported financially for MSc Thesis Project by Istanbul Technical University Scientific Research Projects Foundation ITU BAP with Project ID: 44249.

References

1. Bel T, Cakar H, Yahya N, Arslan C, Baydogan N (2017) Defect and Diffusion Forum (227–231). Trans Tech Publications, Switzerland
2. Khan WS, Hamadneh NN, Khan WA (2017) Science and Applications of Tailored Nanostructures. One Central Press, USA
3. Umar Ali (2015) Khairil Juhanni Bt. Abd Karim Nor Aziah Buang. Polym Rev 678–705. https://doi.org/10.1080/15583724.2015.1031377
4. Alqahtani M (2020) J Mech Behav Biomed Mater 110:103937
5. Zhang Y, Zhuang S, Xiaoyong Xu, Jingguo Hu (2013) Opt Mater 36(2):169–172
6. Kim SC, Choi JR (2019) Radiation effects and defects in solids 284–293
7. Bel T, Arslan C, Baydogan N (2018) Mater Chem Phys 221:58–67

8. Eshwar P (2016) IOSR Journal of Mechanical and Civil Engineering (IOSR-JMCE, 13, 2 Ver. I (1–4)
9. Kiran MSRN, Raidongia K, Ramamurty U, Rao CNR (2011) Scripta Mater 64(6):592–595
10. Yifei Y, Lin Z, Lijie H, Wei W, Guanhui M (2011) J Solid State Chem 184(12):3364–3367
11. Bel T, Muhammettursun M, Kocacinar E, Erman E, Gul FB, Dogan E, Celep M, Baydogan N (2021) J Appl Polym Sci 138. https://doi.org/10.1002/app.50897
12. Muhammettursun M, Bel T, Kocacinar E, Erman E, Gul FB, Augousti AT, Baydogan N (2021) J Appl Polym Sci 50689. https://doi.org/10.1002/app.20203364
13. Zhi CY, Bando Y, Wang WL, Tang CC, Kuwahara H, Golberg D (2018) Journal of Nanomaterials, 642036, Hindawi Publishing Corporation
14. Pullanchiyodan A, Nair KS, Surendran KP (2017) ACS Omega 2(12):8825–8835
15. Qin L, Li G, Hou J (2015) Xiao yan Yu, Huili Ding, Qingxin Zhang, Nongyue Wang, Xiongwei Qu. Polym Compos 36(9): 1675–1684
16. Sayan P, Sargut ST, Kıran B (2010) Powder Technol 197:254–259
17. Peng J, Dong Y, Wang L, Li L, Li W, Feng H (2014) Industrial and Engineering Chemistry Research 53, 12170 −12178, American Chemical Society
18. Bel T, Yahya N, Cimenoglu H, Arslan C, Baydogan N (2018) J Phys: Conf Ser 1123:012005
19. Liao W, Gu A, Liang G, Yuan L (2012) Colloids and Surfaces A: Physicochemical and Engineering Aspects, 74–82
20. Yigit Y, Kilislioglu A, Karakus S, Baydogan N (2019) Journal of Investigations on Engineering & Technology 2(2):34–39
21. Agrawal G, Negi YS, Pradhan S, Dash M, Samal SK (2017) Characterization of Polymeric Biomaterials, 57–81
22. Gao W, Li Z (2010) Physical Properties and Applications of Polymer Nanocomposites, Woodhead Publishing Series in Composites Science and Engineering, 723–742. https://doi.org/10.1533/9780857090249.4.723
23. Valerio A, Morelhão S (2019) Usage of Scherer's Formula in X-Ray Diffraction Analysis of Size Distribution in Systems of Monocrystalline Nanoparticles. https://doi.org/10.13140/RG.2.2.19196.08327
24. Bel T, Mehranpour S, Sengul AV, Camtakan Z, Baydogan N (2021) J Appl Polym Sci 138:39. https://doi.org/10.1002/app.51337
25. Kocacinar E, Baydogan N (2021) Key engineering materials 897:63–70. https://doi.org/10.4028/www.scientific.net/KEM.897.63
26. Anthony JW, Bideaux RA, Bladh KW, Nichols MC (2003) Handbook of mineralogy, Mineral Data Publishing, Borates, Carbonates, Sulfates, 5, 813, Tucson, Arizona, version 1
27. Bel T, Arslan C, Baydogan N (2019) Mater Chem Phys 221:58–67
28. Suhail AM, Khalifa MJ, Ibrahim OA (2010) Section 7. Atti Della Fondazione Giorgio Ronchi Fondata Da Ronchi, Lucia Ronchi Publisher, Nanotechnology, pp 513–520
29. Grosberg AY, Khokhlov AR (1980) Pierre-Gilles de Gennes, Giant Molecules, 2nd Edition, World Scientific Publishing Co. Pte. Ltd., Singapore
30. Trucillo P, Di Maio E (2021) Review Classification and Production of Polymeric Foams among the Systems for Wound Treatment. Polymers 13:1608. https://doi.org/10.3390/polym13101608
31. Ma Y, Cao X, Feng X, Ma Y, Zou H (2007) Fabrication of superhydrophobic film from PMMA with intrinsic water contact angle below 90. Polymer 48(26):7455–7460. https://doi.org/10.1016/j.polymer.2007.10.038
32. Thukkaram M, Sitaram S, Kannaiyan SK, Subbiahdoss G (2014). Antibacterial efficacy of iron-oxide nanoparticles against biofilms on different biomaterial surfaces. Int J Biomater 2014(716080):6
33. Ngai JHL, Ho JKW, Chan R, Cheung SH, Leung LM, So SK (2017) Growth, characterization, and thin film transistor application of CH3NH3PbI3 perovskite on polymeric gate dielectric layers. RSC Advances 7(78):49353–49360. https://doi.org/10.1039/C7RA08699G
34. Park H, Kim JU, Park S (2012) High-throughput preparation of complex multi-scale patterns from block copolymer/homopolymer blend films Nanoscale, 4(4):2012. https://doi.org/10.1039/c2nr11792d
35. Al-Emam E, Motawea AG, Janssens K, Cae J (2019) Evaluation of polyvinyl alcohol–borax/ agarose (PVA–B/AG) blend hydrogels for removal of deteriorated consolidants from ancient Egyptian wall paintings. Herit Sci 7:22, Springer, 2019
36. Yilmaz EA, Kuntman A (2008) Polimerik yalıtkanlarda yüzey özelliklerinin Temas açısı ile incelenmesi, Elektrik–Elektronik–Bilgisayar Mühendisliği Sempozyumu (ELECO2008), Bursa, Türkiye, Kasim 2008, ss.107–111
37. Dundar N, Candan T, Akbulut Z (2009) Wettability of fire retardant treated laminated veneer lumber (LVL) manufactured from veneers dried at different temperatures, BioResources 4:4, 1536–1544, 2009
38. Dogan T, Bel T, Dogan M, Koken N, Kizilcan N, Baydogan N (2023) High temperature performance adhesive derived from randomly segmented poly (imide siloxane) copolymer. Mater Sci Eng B 287:116160. https://doi.org/10.1016/j.mseb.2022.116160
39. Ojeda JJ, Dittrich M (2012) Methods Mol Biol 881:187–221
40. Gul FB, Danaci E, Baydogan N (2022) Effect of the Improved Bulk Modulus on Dielectric Properties of Poly (methyl methacrylate)/Borax Hybrid Composite at Radar Frequencies. Mater Today Commun 33:104960. https://doi.org/10.1016/j.mtcomm.2022.104960
41. Atala MH, Aygün EBG, Doğan A (2020) Evaluation of the crack formation of feldspathic ceramic reinforced with bor chemicals. J Ceram Process Res 21(4):407–415
42. Kaufmann JE (2019) Enhanced Webassign, ISBN 0538738103, Cengage, NewYork
43. Ersoy A, Kuntman A (2007) Surface properties of polyesters blended with borax mineral. Istanbul University – J Electr Electron Eng 7(2):387 – 391
44. Park EH, Jeong SU, Jung UH, Kim SH, Lee J, Nam SW, Yu YH (2007) Recycling of sodium metaborate to borax. Int J Hydrog Energy 32:2982-2987
45. Sert H, Yıldıran H, Toscalı D (2012) An investigation on the production of sodium metaborate dihydrate from ulexite by using trona and lime. Int J Hydrogen Energy 37(7):5833–5839
46. Chuah HH, Lin-Vien D, Soni U (2001) Poly(trimethyleneterephthalate) molecular weight and Mark–Houwink equation. Polymer 42(16)7137–7139. https://doi.org/10.1016/S0032-3861(01)00043-X
47. Behrouzian F, Razavi SM, Karazhiyan H (2014) Intrinsic viscosity of cress (Lepidium sativum) seed gum: effect of salts and sugars. Food Hydrocolloid 35(2014):100–105. https://doi.org/10.1016/j.foodhyd.2013.04.019
48. Razavi SM, Moghaddam TM, Emadzadeh B, Salehi F (2012) Dilute solution properties of wild sage (Salvia macrosiphon) seed gum. Food Hydrocoll 29(1):205–210
49. Pamies R, Cifre JGH, Martínez MDCL, Torre JG (2018) Determination of intrinsic viscosities of macromolecules and nanoparticles. Comparison of single-point and dilution procedures. Colloid Polym Sci 286(11):1223–1231
50. Iwashita N (2016) Chapter 2, X-Ray Powder Diffraction. Material Science and Engineering of Carbon – Characterization 7–25. Butterworth-Heinemann
51. Bethi B, Sonawane SH (2018) Chapter 12, Nanomaterials and Its Application for Clean Environment. Nanomaterials of Green Energy – Micro and Nano Technologies 385–409
52. Reddy MR, Subrahmanyam AR, Reddy MM, Kumar JS (2016) Materials Today: Proceedings 3:3713–3718
53. Ermurat Y (2021) Journal of Chemist and Chemical Engineers of Croatia 70(1–2):29–38

54. Toboonsung B (2019) Key Eng Mater 798:158–162
55. Fraunhofer JA (2012) International Journal of Dentistry 2012(3):951324
56. Nishino T, Meguro M, Nakamae K, Matsushita AM, Ueda Y (1999) Langmuir 15(13):4321–4323
57. Yuan Y, Lee TR (2013) Surface Science Techniques 3–34
58. Masashi M, Nakajima A, Fujishima A, Hashimoto K, Watanabe T (2010) Langmuir 16(13):5754–5760
59. Waclawska L (1995) J Therm Anal 43:261–269
60. Surudžić R, Jovanović Z, Bıbıć N, Nikolıć B, Mišković-Stanković V (2013) Journal of Serbian Chemical Society 78(12):2087–2098
61. Rajendran S, Uma T (2000) Mater Lett 44(2000):242–247
62. Ramesh S, Leen KH, Kumutha K, Arof AK (2007) Spectrochimica Acta Part A 66:1237–1242
63. Haris MRHM, Kathiresan S, Mohan S, Der, (2010) Pharma Chem 2(4):316–323
64. Thakur VK, Vennerberg D, Madbouly SA, Kessler MR (2013) Royal Society of Chemistry Advances 4:6677–6684
65. Arul KT, Mannam R, Ramachandra Ra MS (2019) Energy harvesting of PZT/PMMA composite flexible films. Curr Appl Phys 19(4):375–380. https://doi.org/10.1016/j.cap.2019.01.003
66. Chen J, Li J, Lirong Xu, Hong W, Yang Y, Chen X (2019) Polymers 11:601
67. Ma Y, Cao X, Feng X, Ma Y, Zou H (2007) Polymers 48:7455–7460
68. Ramya JR, Arul KT, Sathiamurthid P, Nivethaa EAK, Baskara S (2019) Compos B 163:752–760
69. Suzuki S, Ueno K (2016) Langmuir 33(1):138–143
70. Zdziennicka A, Szymczyk K, Krawczyk J, Janczuk B (2017) Appl Surf Sci S0169–4332(17):30068–30075
71. Cui Z, Martinez AP, Adamson DH (2015) Royal Society of Chemistry Publishing 7:22. https://doi.org/10.1039/C5NR00936G
72. Pawde SM, Deshmukh K (2009) J Appl Polym Sci 114:2169–2179
73. Uysal D, Dogan OM, Uysal BZ (2017) Kinetics of Absorption of Carbon Dioxide into Sodium Metaborate Solution. Int J Chem Kinet. https://doi.org/10.1002/kin.21082